Research Article

Thermodynamic and Extrathermodynamic Studies of Enantioseparation of Imidazolinone Herbicides on Chiralcel OJ Column

Wenjian Lao

Department of Environmental Sciences, University of California, Riverside, CA 92521, USA

Correspondence should be addressed to Wenjian Lao; laowjbj@hotmail.com

A homologous series of chiral imidazolinone herbicide was previously resolved on Chiralcel OJ column in high performance liquid chromatography. However, the mechanism of the chiral separation remains unclear. In this study, chromatographic behaviors of five chiral imidazolinone herbicides were characterized by thermodynamic and extrathermodynamic methods in order to enhance the understanding of the chiral separation. Thermodynamic parameters of this study were derived from equilibrium constant (K) that was estimated from the moment analysis of the chromatographic peak. Van't Hoff plots of K ($\ln K$ versus $1/T$) were linear at a range of 15–50°C, only nonlinear at a range of 5–15 °C with n-hexane (0.1%, trifluoroacetic acid)-2-propanol 60/40 (v/v) mobile phase. The enantiomer retention on the chiral column was entropy-driven at a lower temperature (5°C) and enthalpy-driven at a higher temperature (10 to 50°C). Enantioseparations of four of the five imidazolinone herbicides were enthalpy-driven, only entropy-driven for imazaquin. Enantioseparation mechanisms were different in between 5–10°C and 15–50°C probably due to the conformational change of the OJ phase. Enthalpy-entropy compensation showed similar mechanisms in retention and chiral separation for the five $S(-)$ or $R(+)$ enantiomers. Several extrathermodynamic relationships were able to be extracted to address additivity of group contribution.

1. Introduction

Chiral separation in high-performance liquid chromatography (HPLC) is keeping to be of great interest in diverse areas such as the agrochemicals and pharmaceutical industry [1]. To achieve better resolution and improve chiral stationary phase, enantioseparation mechanisms have been studied extensively using various methods [2–4]. A thermodynamic study is found to be especially valuable for providing information on the separation mechanism [5–7]. A link between chromatographic behavior and thermodynamic parameters such as enthalpy ($\Delta H°$), entropy ($\Delta S°$), and Gibbs free energy ($\Delta G°$) is distribution constant (K) that describes the transfer of an analyte from mobile phase to stationary phase [8]. Moment analysis of elution peak based on a kinetic model provides an approach to estimate the K value [9]. The present study is concerned with using the K value to characterize retention and chiral separation, a case where there has been so far few works [10].

Extrathermodynamic relationships are empirical correlations of thermodynamic parameters with molecular structures, chromatographic conditions, and enthalpy-entropy compensation (EEC) and have been among the most important tools in investigation of separation mechanism [11, 12]. Many extrathermodynamic relationships have been developed to facilitate the understanding of chromatographic retention and separation mechanism [13]. Typically, it has been demonstrated that the extrathermodynamic relationship derived from homologous series of analytes with additive group such as methylene or phenyl is able to provide useful information on chromatographic behavior [14, 15]. Since lots of extrathermodynamic relationships such as EEC were established based on thermodynamic parameters, many extrathermodynamic studies were correspondingly implemented with the thermodynamic work [6, 16, 17].

Imidazolinone herbicides including six structurally similar chiral compounds are extensively used in the field.
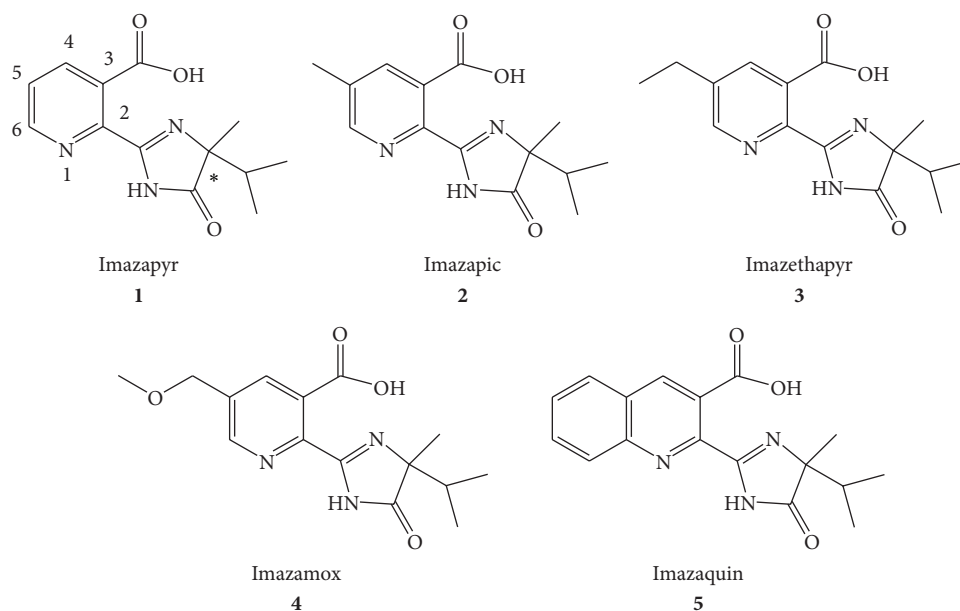
FIGURE 1: Structures of the imidazolinone herbicide.

In a previous study, enantioseparation for five of these compounds was achieved on a Chiralcel OJ column (Figure 1) [18]. The five imidazolinone compounds are a homologous series that has different additive groups on imazapyr (**1**). Although there have been many studies on enantioseparation of OJ column, few studies have been addressed with the effect of temperature and thermodynamic characteristics [19–21]. The main objective of this study was to examine thermodynamic and extrathermodynamic characteristics of chromatographic behaviors for imidazolinone herbicides on the OJ column.

2. Experimental

2.1. Chemicals. Imazapyr (**1**) (99%), imazapic (**2**) (99%), imazethapyr (**3**) (99%), imazamox (**4**) (99%), and imazaquin (**5**) (99%) were purchased from Chem Service (West Chester, PA. USA). Trifluoroacetic acid (TFA) (99%) and 1,3,5-tri-*tert*-butylbenzene (TTBB) (≥97.0%) were obtained from Sigma Aldrich (Milwaukee, WI). Solvents n-hexane and 2-propanol (HPLC grade) were purchased from Fisher (Springfield, NJ, USA).

2.2. Apparatus. All measurements were made on an Agilent 1100 HPLC systems (Agilent, Wilmington, DE, USA). Column temperatures at the range of 15–50°C were controlled by the thermostatic column compartment of the instrument itself. Column temperature at 5 and 10°C was achieved by surrounding the column in a coolant-jacketed cylinder coupled to a thermostat (LAUDA *K-2/R*, Brinkmann Instruments, Germany). The column was a Chiralcel OJ (cellulose 4-methylbenzoate, 250 × 4.6 mm ID with 10 μm particle size, Chiral Technologies, West Chester, PA, USA).

2.3. Chromatography. The analyte concentration was 0.2 mg/mL prepared in the mobile phase. The injection volume was 20 μL. The flow rate of mobile phase was 1.0 mL/min, and the detection wavelength was 254 nm with 4 nm bandwidth. The hold-up time (t_0) of the chromatographic system was measured by TTBB for every temperature and mobile phase composition. The extra volume (t_{ext}) of the instrument system was measured by injecting TTBB solution into the instrument from the pump with a zero-dead volume connector in place of the column. The average t_{ext} value of the Agilent 1100 HPLC system was 0.071 min with n-hexane (0.1%, TFA)-2-propanol 70/30 and 60/40 (v/v) as the mobile phases. The column temperature was changed stepwise at 15, 25, 35, 45, and 50°C for 85/15, 80/20, 75/25, 70/30 and 60/40 (v/v) mobile phases. The column temperatures of 5 and 10°C were only investigated for 70/30, and 60/40 (v/v) mobile phases. The column was equilibrated with the mobile phase for 1 h at each temperature before sample injection. The $S(-)$ enantiomer was first eluted followed by the $R(+)$ enantiomer for all the five imidazolinone herbicides on OJ column [22].

2.4. Data Analysis. In a chromatographic system, retention is related to the change of Gibbs free energy at equilibrium:

$$\ln K = -\frac{\Delta G°}{RT} = -\frac{\Delta H°}{RT} + \frac{\Delta S°}{R}, \tag{1}$$

where $\Delta G°$, $\Delta H°$, and $\Delta S°$ are the differences in the molar Gibbs free energy, the molar enthalpy, and molar entropy, respectively; R is the gas constant; T is the absolute temperature in Kelvin; K is the distribution constant of the solute between stationary phase and mobile phase. According to the moment analysis method, the first absolute moment (μ_1) of

the elution peak equals its retention time (t_R) when the peak profile is symmetrical [11]

$$\mu_1 = t_R = \frac{\int C(t)\, t\, dt}{\int C(t)\, dt} = (t_0 - t_{ext})\left[1 + \frac{1-\varepsilon}{\varepsilon}K\right], \quad (2)$$

where $c(t)$ is the profile of the elution peak and ε is total porosity of the column ($\varepsilon = V_m/V_g = ft_0/0.25\pi d^2 L$, where V_m is the total volume of the mobile phase in the column, V_g is the geometrical volume of the column, f is the mobile phase flow rate, d is the diameter of the column tube, and L is the length of the column). From (2), K is given by

$$K = \frac{C_s}{C_m} = \frac{k}{\Phi} = \frac{t_R - (t_0 - t_{ext})}{(t_0 - t_{ext})}\frac{\varepsilon}{1-\varepsilon}, \quad (3)$$

where C_s and C_m are the concentration of the solute in the stationary phase and mobile phase at equilibrium, respectively, k is retention factor, and Φ is column phase ratio.

When enantioseparation is achieved with a separation factor α, the difference in enthalpy and entropy of the two enantiomers is given by

$$\ln \alpha = \ln \frac{k_2}{k_1} = \ln \frac{K_2}{K_1} = -\frac{\Delta(\Delta H^\circ)}{RT} + \frac{\Delta(\Delta S^\circ)}{R}. \quad (4)$$

For nonlinear van't Hoff behavior, dependence of $\ln K$ and $1/T$ can be estimated by a quadratic form

$$\ln K = A + \frac{B}{T} + \frac{C}{T}, \quad (5)$$

where the coefficients A, B, and C can be estimated by nonlinear regression methods. ΔH° and ΔS° can then be obtained by

$$\begin{aligned}\Delta H^\circ &= -R\left(B + \frac{2C}{T}\right),\\[1mm] \Delta S^\circ &= R\left(A - \frac{C}{T^2}\right).\end{aligned} \quad (6)$$

Equations (6) show that ΔH° and ΔS° are temperature dependent with nonlinear van't Hoff behavior [12].

The EEC phenomenon has been used to estimate the retention and enantioseparation mechanisms of chromatographic systems [7–9]. The EEC on the retention is expressed by

$$\Delta H^\circ = \beta \Delta S^\circ + \Delta G_\beta^\circ, \quad (7)$$

where ΔG_β° is the Gibbs free energy at a compensation temperature β. The EEC on the separation factor can be expressed as

$$\Delta(\Delta H^\circ) = \beta\Delta(\Delta S^\circ) + \Delta(\Delta G^\circ)_\beta. \quad (8)$$

At the compensation temperature of separation factor, separation factor α is given by

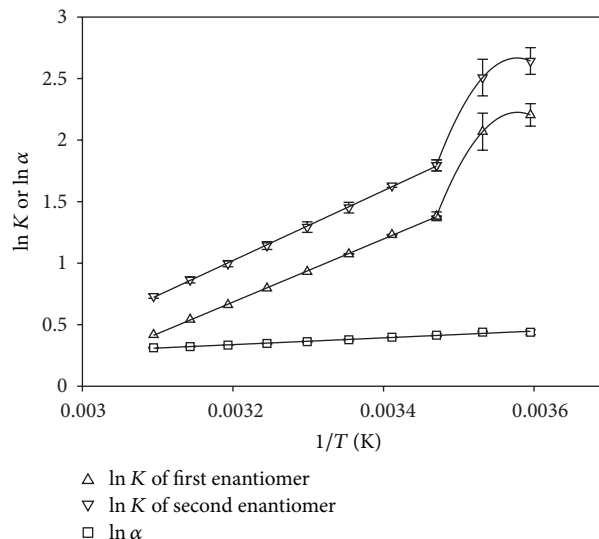$$\ln \alpha_\beta = -\frac{\Delta(\Delta G_\beta^\circ)}{RT_\beta}. \quad (9)$$

FIGURE 2: Van't Hoff plots of K and α of imazamox at range of 5–50°C with 60/40 mobile phase.

△ $\ln K$ of first enantiomer
▽ $\ln K$ of second enantiomer
□ $\ln \alpha$

If the EEC is observed, it just means that the retention or enantioseparation may be similar. Reversely, an obvious different EEC can certify different retention or enantioseparation mechanisms [23]. Applying Martin's additive-free-energy relationship [13], a functional group contribution to thermodynamic quantities can be written as

$$\begin{aligned}\Delta(\Delta H_e^\circ)_{i-j} &= (\Delta H_e^\circ)_i - (\Delta H_e^\circ)_j,\\[1mm] \Delta(\Delta S_e^\circ)_{i-j} &= (\Delta S_e^\circ)_i - (\Delta S_{e1}^\circ)_j, \\[1mm] \Delta(\Delta G_e^\circ)_{i-j} &= (\Delta G_e^\circ)_i - (\Delta G_e^\circ)_j,\end{aligned} \quad (10)$$

where subscript e represents S ($e = 1$) or R ($e = 2$) enantiomer and i and j represent the different imidazolinone herbicides.

3. Results and Discussion

3.1. Effect of Molecular Structure on Thermodynamic Parameters.
Van't Hoff plots of K and α were linear within 15–50°C. Nonlinear van't Hoff plots of K were obtained only at range of 5–15°C with 60/40 (v/v) mobile phase (Figure 2).

3.1.1. Thermodynamic Parameters at 15–50°C.
Generally, values of ΔH°, ΔS°, and ΔG° were negative for all the enantiomers (Table 1), suggesting that their retentions were enthalpy-driven. The first-eluted $S(-)$ enantiomer of imazapyr (1) presented the highest ΔH° value among the five compounds with 85/15 mobile phase. When the hydrogen atom at C5 position of imazapyr (1) pyridine ring (Figure 1) was substituted by a methyl and an ethyl group to form imazapic (2) and imazethapyr (3), the ΔH° decreased by 1.4 and 0.9 kJ mol^{-1}, respectively. The smallest ΔH° belonged to imazamox (4), which was less by 3.2 kJ mol^{-1} than imazapyr (1). Imazaquin (5) had almost equal ΔH° to imazapyr (1). On the other hand, the variation of ΔH° for the $R(+)$ enantiomer

TABLE 1: Thermodynamic parameters of the imidazolinone herbicides.

Compound	Mobile phase	ΔH°_S kJ mol^{-1}	ΔH°_R kJ mol^{-1}	ΔS°_S J mol^{-1} K^{-1}	ΔS°_R J mol^{-1} K^{-1}	$\Delta G^{\circ}_{S(303\,K)}$ kJ mol^{-1}	$\Delta G^{\circ}_{R(303\,K)}$ kJ mol^{-1}
Imazapyr	85/15	−22.56	−27.02	−51.07	−60.86	−7.08	−8.58
	80/20	−21.10	−25.64	−50.66	−60.91	−5.75	−7.19
	75/25	−20.48	−24.89	−52.19	−62.22	−4.66	−6.04
	70/30	−20.60	−25.06	−55.38	−65.70	−3.82	−5.16
	60/40	−18.19	−21.97	−51.89	−60.32	−2.47	−3.69
Imazapic	85/15	−24.00	−27.50	−57.42	−64.62	−6.60	−7.92
	80/20	−22.56	−26.02	−56.84	−64.08	−5.33	−6.61
	75/25	−21.83	−25.29	−57.86	−65.23	−4.30	−5.53
	70/30	−21.87	−25.52	−60.60	−68.71	−3.50	−4.70
	60/40	−19.57	−22.64	−57.25	−63.71	−2.23	−3.34
Imazethapyr	85/15	−23.42	−25.19	−58.68	−61.22	−5.64	−6.64
	80/20	−21.96	−23.74	−57.96	−60.67	−4.40	−5.36
	75/25	−21.22	−23.08	−58.83	−61.94	−3.39	−4.31
	70/30	−21.26	−23.12	−61.48	−64.71	−2.63	−3.51
	60/40	−19.06	−20.66	−58.22	−60.85	−1.42	−2.22
Imazamox	85/15	−25.73	−27.19	−60.95	−62.19	−7.26	−8.35
	80/20	−24.49	−26.00	−61.19	−62.78	−5.95	−6.98
	75/25	−23.99	−25.58	−63.11	−65.06	−4.87	−5.86
	70/30	−24.17	−25.85	−66.43	−68.81	−4.04	−5.00
	60/40	−21.92	−23.45	−63.38	−65.50	−2.72	−3.60
Imazaquin	85/15	−23.26	−23.40	−51.45	−50.23	−7.67	−8.18
	80/20	−21.84	−21.97	−51.15	−49.95	−6.34	−6.84
	75/25	−21.11	−21.23	−52.34	−51.14	−5.25	−5.73
	70/30	−21.08	−21.19	−55.01	−53.84	−4.41	−4.87
	60/40	−17.81	−17.83	−48.86	−47.49	−3.01	−3.44

Subscripts S and R denote the $S(-)$ and $R(+)$ enantiomers. Chromatographic conditions: Chiralcel OJ column; flow rate, 1 mL/min; detection wavelength, 254 nm; mobile phase, n-hexane (0.1%TFA)-2-propanol (v/v); column temperature, 15–50°C.

was different from the $S(-)$ enantiomer. Imazaquin (5) had the highest ΔH° value. Values of ΔS° for the $S(-)$ enantiomers decreased in an order of imazapyr (1) ≈ imazaquin (5) > imazapic (2) > imazethapyr (3) > imazamox (4) with 85/15 (v/v) mobile phase. Values of ΔS° for the $R(+)$ enantiomer of imazapyr (1), imazapic (2), imazethapyr (3), and imazamox (4) were all less than their $S(-)$ enantiomers, but only imazaquin (5) was reversed.

The high ΔS° of imazapyr (1) suggested that its enantiomers had large movement freedom in chiral cavity of the OJ phase, likely due to its smaller molecular size [24]. The lowest value of ΔS° for imazapic (2) $R(+)$ enantiomer indicated that it is possible to fit in the chiral cavity better than the other enantiomers. The highest ΔS° for imazaquin (5) could be resulted from its bulk molecular size which diminishes the fitting degree to the chiral cavity. Consequently, the effect of steric factor appeared to play an important role in enantiorecognition on the OJ column [25].

Imazaquin (5) had positive $\Delta(\Delta S^{\circ})$ and a very small $-\Delta(\Delta H^{\circ})$ indicating that its chiral separation was entropy-driven (Table 2). The other four herbicides had negative values for both $\Delta(\Delta H^{\circ})$ and $\Delta(\Delta S^{\circ})$ suggesting enthalpy-driven chiral separations. The decrease of $-\Delta(\Delta H^{\circ})$ and $-\Delta(\Delta S^{\circ})$ followed an order imazapyr (1) > imazapic (2) >

imazethapyr (3) > imazamox (4) > imazaquin (5), which was consistent with the increase of substituent dimension on the pyridine ring. The decrease in $-\Delta(\Delta G^{\circ})$ followed a similar trend to that for $-\Delta(\Delta H^{\circ})$ or $-\Delta(\Delta S^{\circ})$, with the exception for imazethapyr (3) and imazamox (4). With the entropy compensation, $-\Delta(\Delta G^{\circ})$ of imazamox (4) was larger than that of imazethapyr (3). The value of $-\Delta(\Delta H^{\circ})$ for imazaquin (5) was very small, which reflected a poor steric fitness to the CSP. However, the positive $\Delta(\Delta S^{\circ})$ made a counterbalance to achieve the enantioseparation.

In order to evaluate the relative contribution of enthalpy and entropy to the enantioseparation, enthalpy-entropy ratio Q [$Q = \Delta(\Delta H^{\circ})/(303 \times \Delta(\Delta S^{\circ}))$] at 303 K was calculated (Table 2) [26]. The calculated Q followed an order of imazamox (4) > imazethapyr (3) > imazapic (2) > imazapyr (1) > imazaquin (5). The Q values of imazapyr (1), imazapic (2), imazethapyr (3), and imazamox (4) were positive and greater than 1, indicating the larger molecule for imazamox (4), imazethapyr (3), imazapic (2), and imazapyr (1), the greater contribution to enthalpy. Imazaquin (5) had a positive Q value, revealing that the large and rigid quinoline moiety may exert a different effect on solute-CSP complexation to cause a greater entropic contribution [27].

TABLE 2: Thermodynamic parameters $\Delta\Delta H°$, $\Delta\Delta S°$, and $\Delta\Delta G°_{(303\,K)}$ of chiral separation.

Compound	Mobile phase	$\Delta\Delta H°$ kJ mol^{-1}	$\Delta\Delta S°$ J mol^{-1} K^{-1}	$\Delta\Delta G°_{(303\,K)}$ kJ mol^{-1}	$Q^*_{(303\,K)}$
Imazapyr	85/15	−4.47	−9.80	−1.50	1.50
	80/20	−4.54	−10.25	−1.44	1.46
	75/25	−4.42	−10.03	−1.38	1.45
	70/30	−4.46	−10.32	−1.33	1.43
	60/40	−3.78	−8.43	−1.23	1.48
Imazapic	85/15	−3.51	−7.20	−1.32	1.61
	80/20	−3.47	−7.24	−1.27	1.58
	75/25	−3.46	−7.36	−1.23	1.55
	70/30	−3.66	−8.11	−1.20	1.49
	60/40	−3.07	−6.46	−1.11	1.57
Imazethapyr	85/15	−1.77	−2.54	−1.00	2.30
	80/20	−1.78	−2.71	−0.95	2.16
	75/25	−1.85	−3.11	−0.91	1.97
	70/30	−1.85	−3.23	−0.88	1.90
	60/40	−1.60	−2.63	−0.80	2.01
Imazamox	85/15	−1.45	−1.23	−1.08	3.89
	80/20	−1.51	−1.58	−1.03	3.15
	75/25	−1.58	−1.95	−0.99	2.68
	70/30	−1.68	−2.38	−0.96	2.33
	60/40	−1.53	−2.12	−0.89	2.38
Imazaquin	85/15	−0.14	1.22	−0.51	
	80/20	−0.13	1.19	−0.49	
	75/25	−0.11	1.20	−0.48	
	70/30	−0.11	1.18	−0.46	
	60/40	−0.02	1.37	−0.44	

*Enthalpy-entropy ratios Q, relative contribution of enthalpy and entropy to the enantioseparation at 303 K.

TABLE 3: Temperature dependence of thermodynamic parameters with n-hexane (0.1%TFA)-2-propanol 60/40 (v/v) as mobile phase.

Compound	Temperature (°C)	$\Delta H°_S$	$\Delta H°_R$	$\Delta S°_S$	$\Delta S°_R$	$\Delta G°_S$	$\Delta G°_R$
Imazapyr	5	26.20	35.36	110.20	148.37	−4.44	−5.89
	10	−48.55	−49.26	−156.29	−153.32	−5.10	−6.64
Imazapic	5	30.30	22.62	124.43	101.60	−4.29	−5.62
	10	−50.12	−52.45	−162.29	−166.06	−5.00	−6.28
Imazethapyr	5	35.02	37.19	138.38	149.63	−3.45	−4.40
	10	−49.25	−51.14	−162.05	−165.32	−4.20	−5.18
Imazamox	5	22.99	25.09	100.97	112.16	−5.08	−6.09
	10	−53.93	−55.49	−173.26	−175.12	−5.76	−6.80
Imazaquin	5	29.29	31.80	123.25	133.58	−4.97	−5.34
	10	−47.13	−46.10	−149.20	−144.14	−5.65	−6.03

3.1.2. Thermodynamic Parameters at 5–15°C. The nonlinear van't Hoff plots in the range of 5–15°C caused temperature-dependent thermodynamic profile according to (6) (Table 3). The $\Delta H°$ and $\Delta S°$ values were negative at 10°C but positive at 5°C with 60/40 mobile phase, indicating that the retention of enantiomers was entropy-driven at 5°C and enthalpy-driven from 10 to 50°C. For enantioselective separation, positive values of $\Delta(\Delta H°)$ and $\Delta(\Delta S°)$ at 5°C for imazapyr (**1**), imazethapyr (**3**), imazamox (**4**), and imazaquin (**5**)

suggest entropy-driven (Table 4). The $\Delta(\Delta H°)$ and $\Delta(\Delta S°)$ of imazapic (**2**) were negative at 5 to 10°C. At 10°C, imazapyr (**1**) and imazaquin (**5**) had positive $\Delta(\Delta S°)$.

Nonlinear van't Hoff behaviors have been observed in many studies, for example, enantioseparation of dihydropy-rimidinone on Chiralcel AD column [28], and a diol compound on Chiralcel OJ column [19]. Since small analytes were used, the AD and OJ phases based on polysaccharide were concluded to undergo thermally induced conformational

TABLE 4: Temperature dependence of thermodynamic parameters for chiral separation with n-hexane (0.1%TFA)-2-propanol 60/40 (v/v) as mobile phase.

Compound	Temperature (°C)	$\Delta\Delta H°$ kJ mol^{-1}	$\Delta\Delta S°$ J mol^{-1} K^{-1}	$\Delta\Delta G°$ kJ mol^{-1}	Q
Imazapyr	5	9.16	38.16	−1.45	0.86
	10	−0.71	2.97	−1.54	
Imazapic	5	−7.68	−22.83	−1.33	1.21
	10	−2.33	−3.77	−1.28	2.19
Imazethapyr	5	2.18	11.25	−0.95	0.70
	10	−1.90	−3.27	−0.99	2.05
Imazamox	5	2.10	11.19	−1.01	0.67
	10	−1.56	−1.86	−1.04	2.97
Imazaquin	5	2.51	10.33	−0.36	0.87
	10	1.03	5.07	−0.38	0.72

TABLE 5: The correlation coefficients (r^2), compensation temperature (β) and $\Delta G°_\beta$ in enthalpy-entropy compensation.

Mobile phases	$(r^2)_S$	β (°C)	$\Delta G°_\beta$	$(r^2)_R$	β (°C)	$\Delta G°_\beta$
85/15	0.668	−16.0	−11.44	0.812	45.0	−9.19
80/20	0.718	2.2	−9.10	0.837	53.4	−7.34
75/25	0.757	16.8	−7.29	0.860	57.4	−6.02
70/30	0.788	25.7	−6.09	0.888	64.2	−4.76
60/40	0.877	29.7	−4.40	0.927	61.9	−3.50

changes. On the other hand, nonlinear van't Hoff plots are usually observed for polymeric analytes such as polypeptide and protein due to their interactions with nonpolar n-alkyl stationary phase in hydrophobic environments. These nonlinear van't Hoff plots were a result of the conformational changes of analytes [12]. However, nonlinear van't Hoff plots were also found for small analyte on a small molecule stationary phase derived from (R)-N-(3,5-dinitrobenzoyl) phenylglycine. This unusual behavior was assigned to the temperature-dependent interaction of 2-propanol with the stationary phase and/or the analyte [29]. It showed thereby that the origin of the nonlinear van't Hoff behaviors may result from conformational changes of stationary phases, analyte, or their combinations. In the case of this study, more likely, the conformation change of the OJ phase caused the nonlinear van't Hoff plots under the low temperature [19].

3.2. Effect of Mobile Phase Composition on Thermodynamic Parameters.

Changes of $\Delta H°$ for both of enantiomers followed the same trend. Generally, the $\Delta H°$ increased with increasing 2-propanol concentration from 15% to 40% (v/v) (Table 1). The differences of $\Delta H°$ between using 15% and 40% 2-propanol concentrations were, respectively, 3.8 and 3.7 kJ mol^{-1} for the first- and second-eluted enantiomers of imazamox (4), which were the smallest changes among the five compounds. The corresponding differences were 5.5 and 5.6 kJ mol^{-1} for imazaquin (5), the greatest $\Delta H°$ variations among the five compounds.

The overall dependence of $\Delta S°$ on the 2-propanol content was different from the $\Delta H°$. The $\Delta S°$ values increased with 2-propanol concentration increasing from 15 to 20%, decreased from 20 to 30%, and then increased again from 30 to 40%. The minimum $\Delta S°$ values for both enantiomers were obtained with 30% 2-propanol.

The effect of 2-propanol concentration on $\Delta(\Delta H°)$ and $\Delta(\Delta S°)$ varied for different compounds. For example, the most negative $\Delta(\Delta H°)$ was observed at 30% 2-propanol content for imazapic (2), imazethapyr (3), and imazamox (4).

At 40% of 2-propanol, $\Delta(\Delta H°)$ of imazaquin (5) became zero, suggesting that the enantioseparation was completely entropy-driven. The $\Delta(\Delta S°)$ decreased with increasing 2-propanol content from 15 to 30% for imazapic (2), imazethapyr (3), and imazamox (4) and then increased with 2-propanol content raising from 30 to 40%. The most negative values of $\Delta(\Delta S°)$ for imazapyr (1), imazapic (2), imazethapyr (3), and imazamox (4) were observed at 30% 2-propanol content. Only imazaquin (5) remained positive $\Delta(\Delta S°)$ over the entire range of 2-propanol content tested. Regardless of the enthalpy or entropy trends, $\Delta G°$ and $\Delta(\Delta G°)$ always increased with the increasing of 2-propanol content.

O'Brien et al. [19] reported that $\Delta(\Delta H°)$, and $\Delta(\Delta S°)$ of a diol compound over a temperate range of 20 to 50°C increased with increasing 2-propanol content from 30% to 45%, which is consistent with our observations for imazapyr (1), imazapic (2), imazethapyr (3), and imazamox (4) over the temperature range of 15 to 50°C and the 2-propanol content range of 30 to 40%. Moreover, the dependences of $\Delta H°$, $\Delta S°$, $\Delta(\Delta H°)$ and $\Delta(\Delta S°)$ on 2-propanol content from 15 to 40% showed that there was a deviation at 30% 2-propanol content. It implied that the conformation of OJ phase not only changed with temperature but also likely with the mobile phase composition [30].

3.3. Enthalpy-Entropy Compensation for Retention and Enantioseparation.

Existence of EEC was revealed by high r^2 (≥0.7) in linear regression between $\Delta H°$ and $\Delta S°$ for the temperature range of 15–50°C (Table 5). The r^2 was consistently greater for the $R(+)$ enantiomer than the $S(-)$ counterpart, indicating that the EEC was more significant for the $R(+)$ enantiomer. The EEC increased with increasing 2-propanol content in the mobile phase. The best correlation (r^2 = 0.927) was observed for the $R(+)$ enantiomer with 60/40 (v/v) mobile phase. The EEC temperature was within the range of −16 to 30°C for the $S(-)$ enantiomer and 45 to 62°C for the $R(+)$ enantiomer.

A plot of $\Delta(\Delta H°)$ versus $\Delta(\Delta S°)$ over the temperature range of 15–50°C yielded r^2 of 0.994 and $\Delta(\Delta G°)_\beta$ of 0.691 (Figure 3), indicating that EEC occurred in the chiral separation. The compensation temperature was 104°C although it is beyond the regular HPLC operational temperature. At this temperature, the separation factor for the five compounds calculated from (11) would be 1.24. The plot of $\Delta(\Delta H°)$ versus $\Delta(\Delta S°)$ over 5–10°C was also linear illustrating EEC existence in the chiral separation (Figure 3). However, different slopes

TABLE 6: $\Delta(\Delta H_e^\circ)_{i-j}$ versus $\Delta(\Delta S_e^\circ)_{i-j}$ associated with various functionary substitutions using 85/15, 80/20, 75/25, 70/30, and 60/40 mobile phases.

| Pairs of compound | Changes of functional group | $S(-)$ | | $R(+)$ | |
	IN/OUT	Slop	r^2	Slop	r^2
Imazapyr-imazapic	CH_3/H	134	0.727	156	0.173
Imazapyr-imazethapyr	CH_3CH_2/H	94	0.401	309	0.515
Imazapyr-imazamox	CH_3OCH_2/H	343	0.998	341	0.999
Imazapyr-imazaquin	C_4H_4/H	318	1	243	0.987
Imazapic-imazethapyr	CH_3CH_2/CH_3	-0.9	0	359	0.857
Imazapic-imazamox	CH_3OCH_2/CH_3	241	0.998	265	0.999
Imazapic-imazaquin	C_4H_4/CH_3	371	0.974	363	0.993
Imazethapyr-imazamox	CH_3OCH_2/CH_3CH_2	202	0.978	221	0.995
Imazethapyr-imazaquin	C_4H_4/CH_3CH_2	397	0.932	393	0.975
Imazamox-imazaquin	C_4H_4/CH_3OCH_2	326	1	304	0.999
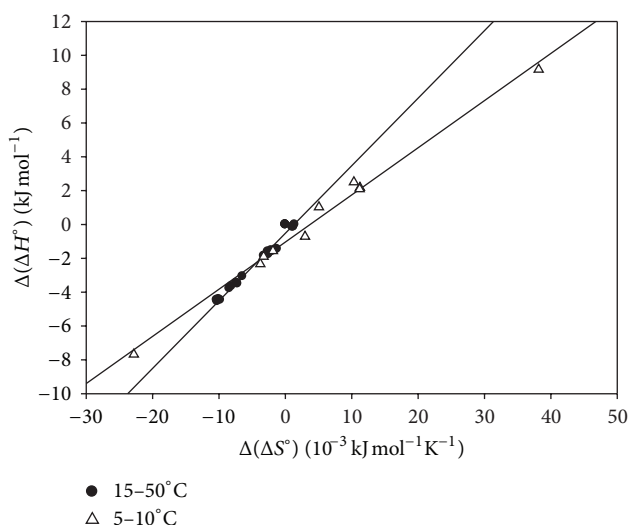
FIGURE 3: Enthalpy-entropy compensation plot of $\Delta(\Delta H^\circ)$ versus $\Delta(\Delta S^\circ)$ at 5–10°C and 15–50°C.

FIGURE 4: Enthalpy-entropy compensation of group selectivity for mobile phase composition.

of the EEC curves confirmed different enantioseparation mechanisms. The EEC phenomenon in the enantioseparation conjoining the analogous chiral structure and the same elution order suggested that the five imidazolinone compounds possibly followed similar enantioseparation mechanism on the OJ column.

3.4. Enthalpy-Entropy Compensation in Additivity of Group Contribution.
EEC associating with functional substitution in the imidazolinone homologous within 15–50°C was described as

$$\Delta\left(\Delta S_e^\circ\right)_{i-j} = m_e \Delta\left(\Delta H_e^\circ\right)_{i-j} + n_e, \tag{11}$$

where m_e and n_e represented the slope and intercept. Results of $\Delta(\Delta H_e^\circ)_{i-j}$ versus $\Delta(\Delta S_e^\circ)_{i-j}$ associated with single functionary substitution across the 85/15, 80/20, 75/25, 70/30, and 60/40 mobile phases are listed in Table 6. In
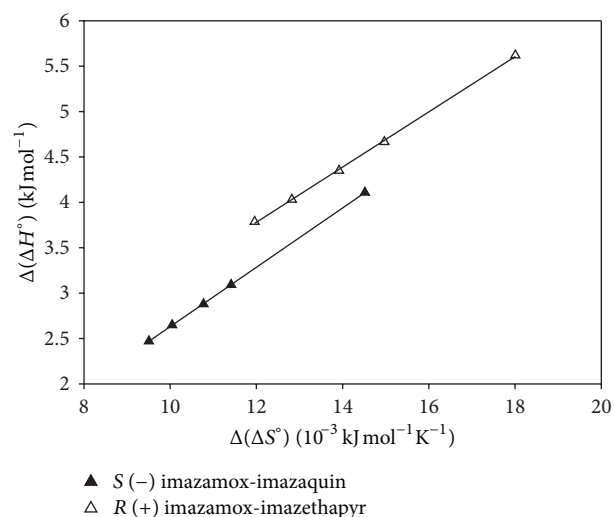
the column of changes of functional group, IN indicates an introduced group, while OUT indicates a replaced group. The large r^2 indicated that EEC of group substitution for $S(-)$ or $R(+)$ enantiomer occurred. For example, good linear correlation relationships of $\Delta(\Delta H_e^\circ)$ versus $\Delta(\Delta S_e^\circ)$ for imazamox (**4**)-imazaquin (**5**), and imazamox (**4**)-imazethapyr (**3**) are plotted in Figure 4. Very weak EEC appeared for $S(-)$ enantiomers among imazapyr (**1**), imazapic (**2**), and imazethapyr (**3**), while $S(-)$ and $R(+)$ imazamox (**4**) impressively showed the EEC interaction with all the other enantiomers.

Results of $\Delta(\Delta H_e^\circ)_{i-j}$ versus $\Delta(\Delta S_e^\circ)_{i-j}$ in single mobile phase, for example, 85/15, across all ten functional substitutions of the homologous series are listed in Table 7. The r^2 for both $S(-)$ and $R(+)$ enantiomers increasing with the increase of 2-propanol concentration revealed that more obvious EEC interactions were induced by the organic modifier. Moreover, the slopes were found having good linear correlation

TABLE 7: Linear correlation relationship of $\Delta(\Delta H_e^\circ)_{i-j}$ versus $\Delta(\Delta S_e^\circ)_{i-j}$ in a single mobile phase across all ten functionary substitutions within the homolog.

2-propanol concentration	S(−)			R(+)		
	Slope m_e	Intercept n_e	r^2	Slope m_e	Intercept n_e	r^2
15%	0.211	−0.45	0.694	0.261	0.274	0.71
20%	0.228	−0.441	0.737	0.276	0.19	0.758
25%	0.243	−0.417	0.775	0.285	0.133	0.805
30%	0.254	−0.393	0.806	0.296	0.087	0.845
35%	0.267	−0.316	0.894	0.295	0.086	0.905

TABLE 8: $\Delta(\Delta G_e^\circ)_{i-j,\,303\,K}$ versus 2-propanol concentration in the mobile phase associated with various functionary substitutions.

Pairs of compound	Changes of functional group IN/OUT	S(−)		R(+)	
		Slop a_φ	r^2	Slop a_φ	r^2
Imazapyr-imazapic	CH_3/H	1.16	0.992	1.48	0.987
Imazapyr-imazethapyr	CH_3CH_2/H	1.92	0.988	2.24	0.981
Imazapyr-imazamox	CH_3OCH_2/H	0.32	0.955	0.72	0.973
Imazapyr-imazaquin	C_4H_4/H	−0.22	0.644	0.74	0.986
Imazapic-imazethapyr	CH_3CH_2/CH_3	0.72	0.973	0.76	0.958
Imazapic-imazamox	CH_3OCH_2/CH_3	0.86	0.988	−0.74	0.992
Imazapic-imazaquin	C_4H_4/CH_3	−1.4	0.959	−0.76	0.958
Imazethapyr-imazamox	CH_3OCH_2/CH_3CH_2	−1.6	0.993	−1.58	0.991
Imazethapyr-imazaquin	C_4H_4/CH_3CH_2	−2.12	0.965	−1.52	0.958
Imazamox-imazaquin	C_4H_4/CH_3OCH_2	−0.54	0.786	0.02	0.011

relationships against the 2-propanol concentration, φ, for $S(-)$ ($r^2 = 0.993$) and $R(+)$ ($r^2 = 0.912$) enantiomers:

$$m_e = c_e\varphi + d_e, \tag{12}$$

where c_e and c_e denote the slop and intercept. The c_e for $S(-)$ enantiomers ($c_e = 0.276$) was larger than for $R(+)$ enantiomers ($c_e = 0.176$). Consequently, an iso-m_e point of $S(-)$ and $R(+)$ enantiomers could be calculated by

$$\varphi = \frac{d_2 - d_1}{c_1 - c_2} \tag{13}$$

to give $\varphi = 60.6\%$. Below this concentration, EEC of the functional substitution was greater for $R(+)$ enantiomer than $S(-)$ and vice versa.

The standard Gibbs energy variation ($\Delta(\Delta G_e^\circ)_{i-j}$) causing from the functional substitution within 15–50°C also showed dependence on φ:

$$\Delta\left(\Delta G_e^\circ\right)_{i-j} = a_\varphi\varphi + b_\varphi, \tag{14}$$

where a_φ and b_φ represented the slop and intercept. Results of linear regression according to (14) for $\Delta(\Delta G_e^\circ)_{i-j}$ at 303 K are listed in Table 8. The large r^2 indicated that the majority of the $\Delta(\Delta G_e^\circ)_{i-j}$ values, except for imazamox (4)-imazaquin (5), exhibited linear dependence on the 2-propanol concentration.

4. Conclusion

The retention of enantiomer was entropy-driven at 5°C and enthalpy-driven at 10 to 50°C. The enantioseparation of imazapyr (1), imazapic (2), imazethapyr (3), and imazamox (4) was enthalpy-driven, whereas chiral separation of imazaquin (5) was entropy-driven. Enantioseparation mechanisms were different between 5–10°C and 15–50°C, which was probably induced by the conformational change of the OJ phase. The EEC showed that the mechanisms of retention and enantioseparation for the five $S(-)$ or $R(+)$ enantiomers were very similar. The EEC in additivity of group contribution concurred with this observation. This study serves as a demonstration to yield useful information by utilizing distribution constant K for understanding enantioseparation mechanism.

Acknowledgment

References

[1] A. Cavazzini, L. Pasti, A. Massi, N. Marchetti, and F. Dondi, "Recent applications in chiral high performance liquid chromatography: a review," *Analytica Chimica Acta*, vol. 706, no. 2, pp. 205–222, 2011.

[2] K. B. Lipkowitz, "Atomistic modeling of enantioselection in chromatography," *Journal of Chromatography A*, vol. 906, no. 1-2, pp. 417–442, 2001.

[3] M. Lämmerhofer, "Chiral recognition by enantioselective liquid chromatography: Mechanisms and modern chiral stationary phases," *Journal of Chromatography A*, vol. 1217, no. 6, pp. 814–856, 2010.

[4] L. Asnin, "Adsorption models in chiral chromatography," *Journal of Chromatography A*, vol. 1269, pp. 3–25, 2012.

[5] H. Kim, K. Kaczmarski, and G. Guiochon, "Thermodynamic analysis of the heterogenous binding sites of molecularly imprinted polymers," *Journal of Chromatography A*, vol. 1101, no. 1-2, pp. 136–152, 2006.

[6] T. Rojkovičová, J. Lehotay, D. Meričko, J. Čižmárik, and D. W. Armstrong, "Study of the mechanism of enantioseparation. IX. Effect of temperature on retention of chiral compounds on a methylated teicoplanin chiral stationary phase," *Journal of Liquid Chromatography and Related Technologies*, vol. 27, no. 16, pp. 2477–2494, 2004.

[7] K. G. Gebreyohannes and V. L. McGuffin, "Thermodynamic and kinetic study of chiral separations of coumarin-based anti-coagulants on derivatized amylose stationary phase," *Journal of Chromatography A*, vol. 1217, no. 38, pp. 5901–5912, 2010.

[8] H. Kim, F. Gritti, and G. Guiochon, "Effect of the temperature on the isotherm parameters of phenol in reversed-phase liquid chromatography," *Journal of Chromatography A*, vol. 1049, no. 1-2, pp. 25–36, 2004.

[9] K. Miyabe, Y. Matsumoto, and G. Guiochon, "Peak parking-moment analysis. A strategy for the study of the mass-transfer kinetics in the stationary phase," *Analytical Chemistry*, vol. 79, no. 5, pp. 1970–1982, 2007.

[10] K. Miyabe and G. Guiochon, "Thermodynamic interpretation of retention equilibrium in reversed-phase liquid chromatography based on enthalpy-entropy compensation," *Analytical Chemistry*, vol. 74, no. 23, pp. 5982–5992, 2002.

[11] K. Miyabet and G. Guiochon, "Extrathermodynamic relationships in reversed-phase liquid chromatography," *Analytical Chemistry*, vol. 74, no. 22, pp. 5754–5765, 2002.

[12] M. T. W. Hearn and G. Zhao, "Investigations into the thermodynamics of polypeptide interaction with nonpolar ligands," *Analytical Chemistry*, vol. 71, no. 21, pp. 4874–4885, 1999.

[13] A. Vailaya and C. Horváth, "Exothermodynamic relationships in liquid chromatography," *Journal of Physical Chemistry B*, vol. 102, no. 4, pp. 701–718, 1998.

[14] T. L. Chester and J. W. Coym, "Effect of phase ratio on van't Hoff analysis in reversed-phase liquid chromatography, and phase-ratio-independent estimation of transfer enthalpy," *Journal of Chromatography A*, vol. 1003, no. 1-2, pp. 101–111, 2003.

[15] E. Grushka, H. Colin, and G. Guiochon, "Retention behavior of alkylbenzenes as a function of temperature and mobile phase composition in reversed-phase chromatography," *Journal of Chromatography A*, vol. 248, no. 3, pp. 325–339, 1982.

[16] L. A. Cole, J. G. Dorsey, and K. A. Dill, "Temperature dependence of retention in reversed-phase liquid chromatography. 2. Mobile-phase considerations," *Analytical Chemistry*, vol. 64, no. 13, pp. 1324–1327, 1992.

[17] L. Asnin, K. Sharma, and S. W. Park, "Chromatographic retention and thermodynamics of adsorption of dipeptides on a chiral crown ether stationary phase," *Journal of Separation Science*, vol. 34, no. 22, pp. 3136–3144, 2011.

[18] W. Lao and J. Gan, "High-performance liquid chromatographic separation of imidazolinone herbicide enantiomers and their methyl derivatives on polysaccharide-coated chiral stationary phases," *Journal of Chromatography A*, vol. 1117, no. 2, pp. 184–193, 2006.

[19] T. O'Brien, L. Crocker, R. Thompson et al., "Mechanistic aspects of chiral discrimination on modified cellulose," *Analytical Chemistry*, vol. 69, no. 11, pp. 1999–2007, 1997.

[20] G. W. Kang, J. H. Ko, and W. J. Cheong, "Thermodynamic study of enantioseparation of arylpropionic acids with a Chiralcel OJ-H stationary phase," *Journal of Liquid Chromatography and Related Technologies*, vol. 28, no. 4, pp. 513–526, 2005.

[21] B. Chankvetadze, "Recent developments on polysaccharide-based chiral stationary phases for liquid-phase separation of enantiomers," *Journal of Chromatography A*, vol. 1269, pp. 26–51, 2012.

[22] M. Los, *The Imidazolinone Herbicides.*, CRC press, Boca Raton, FL, USA, 1991.

[23] R. R. Krug, W. G. Hunter, and R. A. Grieger, "Enthalpy-entropy compensation. 1. Some fundamental statistical problems associated with the analysis of van't hoff and arrhenius data," *Journal of Physical Chemistry*, vol. 80, no. 21, pp. 2335–2341, 1976.

[24] E. Yashima, C. Yamamoto, and Y. Okamoto, "NMR studies of chiral discrimination relevant to the liquid chromatographic enantioseparation by a cellulose phenylcarbamate derivative," *Journal of the American Chemical Society*, vol. 118, no. 17, pp. 4036–4048, 1996.

[25] J. A. Chiarotto and I. W. Wainer, "Determination of metyrapone and the enantiomers of its chiral metabolite metyrapol in human plasma and urine using coupled achiral-chiral liquid chromatography," *Journal of Chromatography B*, vol. 665, no. 1, pp. 147–154, 1995.

[26] W. R. Oberleitner, N. M. Maier, and W. Lindner, "Enantioseparation of various amino acid derivatives on a quinine based chiral anion-exchange selector at variable temperature conditions. Influence of structural parameters of the analytes on the apparent retention and enantioseparation characteristics," *Journal of Chromatography A*, vol. 960, no. 1-2, pp. 97–108, 2002.

[27] L. Limsavarn and J. G. Dorsey, "Influence of stationary phase solvation on shape selectivity and retention in reversed-phase liquid chromatography," *Journal of Chromatography A*, vol. 1102, no. 1-2, pp. 143–153, 2006.

[28] F. Wang, R. M. Wenslow, T. M. Dowling, K. T. Mueller, I. Santos, and J. M. Wyvratt, "Characterization of a thermally induced irreversible conformational transition of amylose tris(3,5-dimethylphenylcarbamate) chiral stationary phase in enantioseparation of dihydropyrimidinone acid by quasi-equilibrated liquid chromatography and solid-state NMR," *Analytical Chemistry*, vol. 75, no. 21, pp. 5877–5885, 2003.

[29] W. H. Pirkle, "Unusual effect of temperature on the retention of enantiomers on a chiral column," *Journal of Chromatography*, vol. 558, no. 1, pp. 1–6, 1991.

[30] A. M. Rizzi, "Band broadening in high-performance liquid chromatographic separations of enantiomers with swollen microcrystalline cellulose triacetate packings. II. Influence of eluent composition, temperature and pressure," *Journal of Chromatography A*, vol. 478, pp. 87–99, 1989.